Pharmacokinetic Comparison To Determine the Mechanisms Underlying the Differential Efficacies of Cationic Diamidines against First- and Second-Stage Human African Trypanosomiasis

Sihyung Yang,[a] Tanja Wenzler,[b,c] Patrik N. Miller,[a] Huali Wu,[d] David W. Boykin,[e] Reto Brun,[b,c] Michael Zhuo Wang[a]

Department of Pharmaceutical Chemistry, School of Pharmacy, University of Kansas, Lawrence, Kansas, USA[a]; Medical Parasitology & Infection Biology, Swiss Tropical and Public Health Institute, Basel, Switzerland[b]; University of Basel, Basel, Switzerland[c]; Department of Pathology and Laboratory Medicine, School of Medicine, The University of North Carolina at Chapel Hill, Chapel Hill, North Carolina, USA[d]; Department of Chemistry, Georgia State University, Atlanta, Georgia, USA[e]

Human African trypanosomiasis (HAT), a neglected tropical disease, is fatal without treatment. Pentamidine, a cationic diamidine, has been used to treat first-stage (hemolymphatic) HAT since the 1940s, but it is ineffective against second-stage (meningoencephalitic, or central nervous system [CNS]) infection. Novel diamidines (DB75, DB820, and DB829) have shown promising efficacy in both mouse and monkey models of first-stage HAT. However, only DB829 cured animals with second-stage infection. In this study, we aimed to determine the mechanisms underlying the differential efficacies of these diamidines against HAT by conducting a comprehensive pharmacokinetic characterization. This included the determination of metabolic stability in liver microsomes, permeability across MDCK and MDR1-MDCK cell monolayers, interaction with the efflux transporter MDR1 (P-glycoprotein 1 or P-gp), drug binding in plasma and brain, and plasma and brain concentration-time profiles after a single dose in mice. The results showed that DB829, an azadiamidine, had the highest systemic exposure and brain-to-plasma ratio, whereas pentamidine and DB75 had the lowest. None of these diamidines was a P-gp substrate, and the binding of each to plasma proteins and brain differed greatly. The brain-to-plasma ratio best predicted the relative efficacies of these diamidines in mice with second-stage infection. In conclusion, pharmacokinetics and CNS penetration influenced the *in vivo* efficacies of cationic diamidines against first- and second-stage HAT and should be considered when developing CNS-active antitrypanosomal diamidines.

Human African trypanosomiasis (HAT; sleeping sickness) is a neglected tropical disease caused by subspecies of *Trypanosoma brucei* and is endemic to sub-Saharan Africa (1). HAT appears in two stages, the hemolymphatic stage (first stage), when parasites are confined to the blood and lymph, and the meningoencephalitic stage (second stage), when parasites infect the central nervous system (CNS), which accounts for the majority of diagnosed cases (2, 3). Without treatment, HAT leads to coma and, eventually, death. Current treatments for second-stage HAT include melarsoprol, eflornithine monotherapy, and nifurtimox-eflornithine combination therapy (NECT). However, these treatments are limited by inconvenient parenteral injections, complex infusion schedules, increasing treatment failure, and/or severe toxicity (1, 3). Hence, new or improved chemotherapeutic agents are needed for second-stage HAT.

Pentamidine, an aromatic diamidine (Fig. 1), has been used to treat first-stage HAT since the 1940s, typically via intramuscular injection (4). However, it is ineffective against second-stage HAT due to low blood-brain barrier (BBB) permeability (5). DB75 (furamidine) is a structural analogue of pentamidine (Fig. 1) and possesses potent *in vitro* antitrypanosomal activities (50% inhibitory concentrations [IC$_{50}$s] of <10 ng/ml against wild-type *T. brucei* strains) that are similar to those of pentamidine (6). Pentamidine and DB75 partially cured mice with acute (first-stage) infection of the *Trypanosoma brucei rhodesiense* STIB900 strain (2/4 and 3/4, respectively, at 4 doses of 20 mg/kg of body weight/day administered intraperitoneally [i.p.]) (6). However, neither of the two drugs was curative in the GVR35 CNS (second-stage) mouse model (unpublished data for pentamidine) (6).

In search of safe and CNS-active antitrypanosomal diamidines,

we synthesized azadiamidines (e.g., DB820 and DB829) (Fig. 1) in which one (or both) benzene ring was replaced by a pyridine ring. DB820 and DB829 had potent *in vitro* antitrypanosomal activities (IC$_{50}$s of <40 ng/ml [or <90 nM] against wild-type *T. brucei* strains), albeit they were less active than pentamidine and DB75 by 2- to 8-fold) (6). However, DB820 and DB829 (at 4 doses of 10 mg/kg/day i.p.) were 100% curative in the STIB900 acute mouse model (6), which was markedly more active than pentamidine and DB75. Moreover, DB829 (at 10 doses of 20 mg/kg/day i.p.) unexpectedly cured all animals in the GVR35 CNS mouse model, where cure was defined as survival for more than 150 days posttreatment without parasitemia relapse (6). Prompted by this observation, DB829 was tested further in the vervet monkey model of second-stage HAT via intramuscular injection, and it cured all infected monkeys (7). As such, DB829 was the first cationic diamidine that cured animals with CNS infections and has been considered a front-running preclinical candidate for the treatment of second-stage HAT (1, 8).

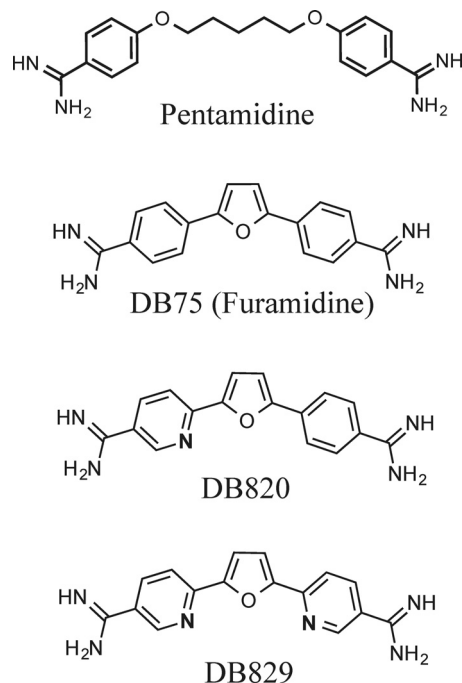To elucidate the mechanisms underlying the differential effi-

FIG 1 Chemical structures of cationic diamidines.

cacies of these cationic diamidines, a comprehensive pharmacokinetic (PK) study was warranted to compare metabolic stability, plasma/tissue binding, BBB permeability, and systemic and brain exposures for pentamidine, DB75, DB820, and DB829. Furthermore, correlations of these measurements with *in vivo* efficacies were made to reveal the properties that best predicted *in vivo* efficacy against first- and second-stage HAT. These results will contribute to the understanding of the *in vivo* drug action of antitrypanosomal diamidines and should be considered when further developing CNS-active diamidines to treat HAT.

MATERIALS AND METHODS

Chemicals. Hydrochloride salts of DB75, DB820, DB829, and deuterated DB75 (DB75-d8; with deuterated phenyl rings) as an internal standard were synthesized as previously reported (9, 10). Pentamidine isethionate was purchased from Sigma-Aldrich (St. Louis, MO). Mouse liver microsomes (MLM; from a pool of 833 male mice) were purchased from Xeno-Tech LLC (Lenexa, KS). Liquid chromatography-tandem mass spectrometry (LC-MS/MS)-grade water, methanol, formic acid, Hanks' balanced salt solution (HBSS) with calcium and magnesium, and HEPES buffer were purchased from Fisher Scientific (Pittsburgh, PA). Lucifer yellow (LY), digoxin, digitoxin, midazolam, D-glucose, dimethyl sulfoxide (DMSO), trifluoroacetic acid, trypsin-EDTA, and NADPH tetrasodium salt were purchased from Sigma-Aldrich. Dulbecco's modified Eagle medium (DMEM) with no glutamine or sodium pyruvate, fetal bovine serum (FBS), penicillin-streptomycin mixtures, L-glutamine, sodium pyruvate, and MEM (minimum essential medium) nonessential amino acids (NEAA) were purchased from Life Technologies (Grand Island, NY).

Animals. Animal study protocols were approved by the Institutional Animal Care and Use Committees (IACUCs) of the University of Kansas and the University of North Carolina at Chapel Hill. Male Swiss Webster mice (20 to 25 g) were purchased from Charles River Laboratories (O'Fallon, MO). Clean room-housed mice were kept under filtered, pathogen-free air in a 12-h light/dark cycle. Food pellets and water were available *ad libitum*.

Cell culture. Madin-Darby canine kidney (MDCK) cells were maintained in DMEM containing 10% (vol/vol) FBS, 1% (vol/vol) NEAA, 1 mM sodium pyruvate, 4 mM L-glutamine, and penicillin-streptomycin (100 units of penicillin and 100 μg of streptomycin per ml) and cultured at 37°C under 5% CO_2 and 95% relative humidity. Cells were passaged at 80 to 90% confluence using trypsin-EDTA solution.

pK_a, $logD_{7.4}$, and metabolic stability determinations. The pK_a and $logD_{7.4}$ (logarithm of distribution constant at pH 7.4) values of each diamidine were experimentally measured by *p*ION Inc. (Woburn, MA) using a spectrophotometric method with methanol as a cosolvent (11). Metabolic stability was evaluated using MLM supplemented with NADPH. Microsomal incubations were carried out as described previously (12), with modifications. Briefly, diamidines were dissolved in water and added to the incubation buffer to achieve final concentrations of 1.0 and 10 μM, which represented plasma concentrations observed in the mouse pharmacokinetic study described below. The microsomal protein concentration was 0.5 mg/ml during incubation. Reactions (in triplicate) were allowed to proceed for up to 60 min at 37°C and were quenched with 20 volumes (vol/vol) of 7:1 (vol/vol) methanol/water containing 0.1% (vol/vol) trifluoroacetic acid and 10 nM internal standard (DB75-d8). After centrifugation, the supernatants were analyzed by ultra-performance LC (UPLC)-MS/MS to quantify the amount of substrate remaining. Pafuramidine (DB289) served as a positive control for microsomal catalytic activity (13). Microsomal half-life ($t_{1/2}$) values were obtained by fitting percentage of substrate remaining-time curves to the one-phase exponential decay equation ($C = C_0 \times e^{-k \cdot t}$; $t_{1/2} = 0.693/k$), where C_0, k, and t are initial concentration, rate constant, and time, respectively.

BBB permeability and P-gp-mediated efflux assays. To compare the permeability of diamidines across the BBB, the MDR1-transfected MDCK (MDR1-MDCK) cell monolayer model was chosen as an *in vitro* BBB model due to its simplicity and its similar predictability when compared to other existing *in vitro* models that use cells derived from brain endothelium (14–16). The bidirectional permeabilities, apical-to-basolateral (A-B) and basolateral-to-apical (B-A), of diamidines across the wild-type (WT) MDCK and MDR1-MDCK cell monolayers were determined as described previously (17). Briefly, transwell inserts (12-mm diameter and 0.4-μm pore size; Corning, Inc., Tewksbury, MA) were preincubated with culture medium for 1 h at 37°C and then seeded with 2×10^5 cells/ml (0.5 ml per insert well). MDCK cell monolayers were cultured for 5 to 7 days before use. Permeability assays (in triplicate) were initiated by replacing medium in the donor chamber with transport medium containing a test compound. The transport medium consisted of HBSS containing 10 mM HEPES and 25 mM D-glucose at pH 7.4. The compound concentrations in the donor chamber were 1 and 10 μM for diamidines (representative of plasma concentrations observed in the mouse pharmacokinetic study described below), 500 μg/ml for LY (paracellular integrity marker), and 10 μM for digoxin (P-glycoprotein [P-gp] marker substrate). After 1 h of incubation at 37°C in a tissue culture incubator (transport was linear within 1 h; data not shown), samples were removed from both apical and basolateral chambers and analyzed for diamidine, digoxin, and midazolam concentrations by UPLC-MS/MS. LY concentrations were measured using a fluorescence microplate reader (FL600; Bio-Tek, Winooski, VT) with excitation and emission wavelengths of 485 and 530 nm, respectively. Transepithelial electrical resistance (TEER) values were measured for each insert to confirm the integrity of the monolayers. Only samples with acceptable TEER values ($>130 \ \Omega \cdot cm^2$) were used for analysis. Apparent permeability (P_{app} [cm/s]) was calculated as follows: $P_{app} = [V_r/(S \times C_0)] \times dC_r/dt$, where V_r is the volume of medium (ml) in the receiver chamber, S is the surface area (cm^2) of the cell monolayer, C_0 is the initial concentration (μM) of the compounds in the donor chamber, and dC_r/dt is the linear slope of the compound concentration in the receiver chamber over time (μM/s). Efflux ratios (R_E) were calculated as the ratio of $P_{app,B-A}$ over $P_{app,A-B}$. Net flux ratios were calculated by dividing the efflux ratio in MDR1-MDCK cells by that in WT MDCK cells; a ratio greater than 2 is indicative of a P-gp substrate according to FDA guidance (18). Mass bal-

ance (%), defined as the percentage of the amount of compound recovered in the apical and basolateral chambers relative to the initial amount in the donor chamber, was calculated for each transport study as follows: mass balance (%) = $\{[(C_d \times V_d) + (C_r \times V_r)]/(C_0 \times V_d)\} \times 100$, where V_d is the volume of medium (ml) in the donor chamber, V_r is the volume of medium (ml) in the receiver chamber, C_d and C_r are the compound concentrations (μM) in the donor and receiver chambers, respectively, and C_0 is the initial compound concentration (μM) in the donor chamber.

Plasma and tissue binding assays. The binding of cationic diamidines to mouse plasma and brain was evaluated by the equilibrium dialysis method using the rapid equilibrium dialysis device (Thermo Scientific Pierce, Rockford, IL) as described previously (19). Briefly, blank (untreated) mouse brains were collected and homogenized in two volumes (vol/wt) of water (3-fold dilution). Diamidines were spiked into blank plasma or brain homogenates to give final drug concentrations of 1 and 5 μM. Spiked plasma or brain homogenates were added to the dialysis device and dialyzed against phosphate-buffered saline (PBS) for 6 h at 37°C to reach equilibrium between the plasma/tissue compartment and the buffer compartment. At the end of the incubation, samples from the plasma/tissue compartment and the buffer compartment were collected and analyzed for total (bound plus unbound) and unbound drug concentrations, respectively, by UPLC-MS/MS. Unbound fractions in the mouse brain ($f_{u,\text{brain}}$) were calculated by correcting for dilution using the following equation (20): $f_{u,\text{brain}} = (1/D)/\{[(1/f_{u,\text{dilute}}) - 1] + 1/D\}$, where D is the dilution factor for the mouse brain homogenates ($D = 3$) and $f_{u,\text{dilute}}$ is the unbound fraction measured in the mouse brain homogenates.

Pharmacokinetics and brain exposure. The single-dose pharmacokinetics of each cationic diamidine were evaluated in mice (in triplicate) after intravenous (i.v.), oral (*per os* [p.o.]), and i.p. administration. The compounds were first dissolved in sterile water and then further diluted to the desired concentrations with saline (1:1, vol/vol) to avoid precipitation when added directly to saline. The doses were 7.5 μmol/kg for i.v. administration, 100 μmol/kg for p.o. administration, and 65 μmol/kg for i.p. administration. The dose volume was 5 ml/kg. No overt adverse effects were observed in mice at these dose levels. These doses were either the same or similar to those used in previous efficacy studies in mice (6, 8). Blood sampling was done at 0.25, 0.5, 1, 2, 4, 6, 8, 12, 24, 48, and 72 h postdose. Additional earlier sampling times of 0.0167 and 0.083 h for i.v. administration of DB829 and pentamidine and 0.083 h for i.v. administration of DB75 and DB820 were included. Blood (~40 μl per bleed) was collected via the submandibular vein or heart into lithium heparin-coated Microvet tubes (Sarstedt, Inc., Newton, NC). Terminal blood and brain samples were collected at 4, 12, and 72 h after i.p. dose. Plasma was obtained by centrifugation. Excised mouse brain samples were quickly rinsed with distilled water, blotted dry with tissue paper, and weighed. All samples were stored at −20°C until further processing for quantification by UPLC-MS/MS.

Sample preparation and UPLC-MS/MS analysis. Thawed mouse brain samples were mixed with two volumes (vol/wt) of water and homogenized using a sonic dismembrator (Fisher Scientific, Fair Lawn, NJ). Plasma (2 μl) or brain homogenate (10 μl) samples were mixed with 200 μl of 7:1 (vol/vol) methanol/water containing 0.1% (vol/vol) trifluoroacetic acid and DB75-d8 (5 nM; internal standard), followed by centrifugation to pellet precipitated proteins. The supernatants were dried under N_2 at 50°C using a 96-well microplate evaporator (Apricot Designs, Inc., Covina, CA) and reconstituted with 100 μl 15% (vol/vol) methanol containing 0.1% (vol/vol) trifluoroacetic acid prior to UPLC-MS/MS analysis. Samples from equilibrium dialysis, metabolic stability, and transport studies were treated like the plasma and brain homogenate samples and processed as described above.

The quantification of diamidines, digoxin, and midazolam was performed on a Waters Xevo TQ-S triple-quadrupole mass spectrometer (Foster City, CA) coupled with a Waters Acquity UPLC I-class system. The analytical conditions for DB75 and DB820 were the same as those for

pentamidine and DB829 and were described previously in detail (8). The characteristic single-reaction monitoring (SRM) transitions for pentamidine, DB75, DB820, DB829, and DB75-d8 were m/z 341.4→120.1, 305.2→288.1, 306.2→272.1, 307.1→273.1, and 313.2→296.3, respectively, under positive electrospray ionization mode. The calibration curves for the diamidines ranged from 0.005 to 50 μM for plasma samples and from 0.005 to 25 μM for brain homogenate samples. The interday coefficient of variation (CV) and accuracy were determined by measuring the same preparation of three standards three times on three different days; deviations for all diamidines were within ±15%. The SRM transitions for digoxin and digitoxin (internal standard) were m/z 779.7→649.5 and 763.6→633.5, respectively, under negative electrospray ionization mode. The calibration curve for digoxin ranged from 0.005 to 10 μM for transport samples, and the interday CV and accuracy deviations were also within ±15%. The SRM transition for midazolam was m/z 325.1→291.1 under positive electrospray ionization mode, and pentamidine was used as the internal standard. The calibration curve for midazolam ranged from 0.005 to 10 μM for transport samples, and the interday CV and accuracy deviations were also within ±15%.

Pharmacokinetic and statistical analyses. The area under the plasma concentration-time curve from time zero to time infinity ($AUC_{0-\infty}$), terminal elimination half-life ($t_{1/2}$), maximum plasma drug concentration ($C_{\max}$), time to reach $C_{\max}$ ($T_{\max}$), whole body clearance (CL), steady-state volume of distribution (V_{ss}), and mean residence time (MRT) were calculated using the trapezoidal rule-extrapolation method (21) and noncompartmental methods (WinNonlin version 5.3, Pharsight, Mountain View, CA). One-way analysis of variance (ANOVA) with Tukey's *post hoc* test was used to compare the means of permeability or unbound fraction of the four diamidines (GraphPad Prism 5.04; GraphPad Software, Inc., La Jolla, CA). Student's *t* tests (unpaired, two-tailed) were used to compare the mean values for permeability or unbound fraction at two different drug concentrations. Statistical outcomes were considered significant when the *P* value was <0.05.

RESULTS

Physicochemical properties and metabolic stability of cationic diamidines. The pK_a, logP (logarithm of partition coefficient), and $logD_{7.4}$ values for pentamidine, DB75, DB820, and DB829 (Table 1) were experimentally determined using a UV spectrophotometric method (11). Although a slight decrease in pK_a was observed for azadiamidines compared to the values for pentamidine and DB75 (approximately 1 pK_a unit), they were still well above physiologic pH. Hence, like pentamidine and DB75, the azadiamidines DB820 and DB829 remain positively charged under physiologic conditions. Additionally, all four diamidines were metabolically stable in mouse liver microsomes supplemented with NADPH (Table 1). At the longest incubation time (60 min), the percentage of substrate remaining relative to time zero was always greater than 87% for each diamidine (data not shown).

Diamidine permeability across MDR1-MDCK cell monolayers. The BBB permeability of cationic diamidines was assessed using the *in vitro* MDR1-MDCK cell model (Table 1). Two substrate concentrations, 1 and 10 μM, were tested for each diamidine. $P_{\text{app,A-B}}$ across MDR1-MDCK cell monolayers ranged from 1.6×10^{-6} to 4.1×10^{-6} cm/s for the four diamidines. There was no significant difference between the two substrate concentrations tested ($P > 0.05$), except for DB829 ($P = 0.012$). In addition, there was no statistically significant difference among the four diamidines when $P_{\text{app,A-B}}$ was assessed at the 10 μM substrate concentration. The only significant difference observed occurred between DB75 and pentamidine at 1 μM (4.1×10^{-6} versus 1.6×10^{-6} cm/s, respectively). The paracellular marker LY exhibited a low permeability ($P_{\text{app,A-B}} \leq 1.0 \times 10^{-6}$ cm/s), indicating mono-

TABLE 1 Physicochemical properties, metabolic stability, permeability, and net P-gp flux ratios of cationic diamidines[a]

Compound	pK[a]	LogP	LogD[7.4]	Concn (μM)	Microsomal $t_{1/2}$ (min)[b]	MDR1-MDCK $P_{app,A-B}$ (10^{-6} cm/s)	MDR1-MDCK Mass balance (%)	MDR1-MDCK Efflux ratio ($P_{app,B-A}/P_{app,A-B}$)	WT MDCK $P_{app,A-B}$ (10^{-6} cm/s)	WT MDCK Mass balance (%)	WT MDCK Efflux ratio ($P_{app,B-A}/P_{app,A-B}$)	Net flux ratio
Pentamidine	11.60 ± 0.01	1.7 ± 0.1	< −2.0	1	>180	1.6 ± 1.1[d]	99	1.2	0.54 ± 0.40	92	2.2	0.55
				10	>180	1.6 ± 0.60	98	3.1	0.99 ± 0.47	94	4.9	0.63
DB75	11.80 ± 0.01	2.7 ± 0.1	< −2.0	1	>180	4.1 ± 1.1[d]	105	0.5	4.8 ± 0.96[c]	102	0.6	0.83
	10.40 ± 0.03			10	>180	2.5 ± 0.97	96	0.9	1.4 ± 0.52[c]	92	2.4	0.38
DB820	11.03 ± 0.29	1.65 ± 0.13	−4.90	1	>180	2.5 ± 0.42	98	0.8	5.4 ± 1.7	102	0.6	1.3
	10.32 ± 0.15			10	>180	2.8 ± 1.4	96	0.7	3.1 ± 1.3	98	0.9	0.78
DB829	10.35 ± 0.18	1.21 ± 0.20	−4.33	1	>180	2.8 ± 0.30[c]	102	0.8	1.9 ± 0.68	103	0.95	0.84
	9.98 ± 0.16			10	>180	1.8 ± 0.31[c]	102	0.8	2.5 ± 0.99	105	1.3	0.62
Digoxin				10	ND	0.34 ± 0.08	90	25	0.78 ± 0.2	91	6.8	3.7
Midazolam				10	ND	40 ± 6.6	108	0.99	50 ± 2.7	103	1.02	0.97

[a] Values are means ± standard deviations unless otherwise indicated. The $P_{app,A-B}$ values are from triplicate determinations at each concentration.
[b] Microsomal half-lives of diamidines were determined using NADPH-supplemented mouse liver microsomes. ND, not determined.
[c] The difference between the results at 1 and 10 μM was statistically significant ($P < 0.05$).
[d] The difference between the results for pentamidine and DB75 was statistically significant ($P < 0.05$).

layer integrity. The transcellular marker midazolam showed a high permeability ($P_{app,A-B} = 40 \times 10^{-6}$ cm/s) across the MDR1-MDCK cell monolayers, consistent with its high BBB permeability in vivo (15). The overall mass balance ranged from 90% to 108%.

Interaction of diamidines with P-glycoprotein. To assess whether diamidines are substrates of the efflux transporter P-gp, the net flux ratio of each diamidine was determined using WT MDCK and MDR1-MDCK cell monolayers (Table 1). All net flux ratios were less than 2, indicating that none of the four diamidines was a human P-gp substrate. In comparison, digoxin (P-gp marker substrate) showed a net flux ratio of 3.7, similar to the FDA's reference number of 4 (18), demonstrating that P-gp was functionally expressed in the MDR1-MDCK cell monolayers used in our study. The paracellular marker LY exhibited low permeability ($P_{app,A-B} \leq 1.0 \times 10^{-6}$ cm/s), indicating monolayer integrity in all experiments. The overall mass balance ranged between 84% and 105%.

Diamidine binding in plasma and brain. The nonspecific binding of each diamidine to mouse plasma proteins and brain tissues was evaluated at two concentrations, 1 and 5 μM (Table 2). There was no concentration-dependent difference in unbound fractions for any diamidine in mouse plasma or brain, except for the brain unbound fraction ($f_{u,brain}$) of DB820 (0.22% versus 0.40% at 1 and 5 μM, respectively; $P = 0.016$). The plasma unbound fractions ($f_{u,plasma}$) varied significantly between the diamidines (up to 5.9-fold), ranging from 6.8% for DB75 to 40% for DB829 (Table 2). Furthermore, the unbound fractions in brain were considerably lower than those in plasma and varied significantly between diamidines (up to 16-fold), ranging from 0.09% for DB75 to 1.48% for DB829 (Table 2).

Diamidine pharmacokinetics after intravenous and oral administration. The plasma concentration-time profiles of pentamidine, DB75, DB820, and DB829 were determined after a single i.v. dose of 7.5 μmol/kg or a single p.o. dose of 100 μmol/kg (Fig. 2). All profiles exhibited at least a biphasic decline with an initial distribution phase and a terminal elimination phase. The pharmacokinetic outcomes were determined using noncompartmental

analysis (Table 3). Following i.v. administration, DB829 gave the highest AUC and the lowest steady-state volume of distribution (V_{ss}), while pentamidine showed the lowest AUC. The terminal elimination half-life ($t_{1/2}$) ranged from 7.2 h for pentamidine up to 58 h for DB75. Following p.o. administration, little DB75 and DB820 were detected in the plasma ($C_{max} < 0.016$ μM). However, appreciable concentrations of DB829 were detected ($C_{max} = 0.083$ μM), albeit representing merely 1% oral bioavailability (Table 3).

Diamidine pharmacokinetics and brain exposure after intraperitoneal administration. The plasma concentration-time profiles of pentamidine, DB75, DB820, and DB829 were determined after a single 65 μmol/kg i.p. dose of each compound (approximately 20 to 22 mg/kg, depending on the compound's molecular weight) (Fig. 3). All profiles exhibited at least a biphasic decline with an initial distribution phase and a terminal elimination phase. The pharmacokinetic outcomes were determined using noncompartmental analysis (Table 4). DB829 showed the high-

TABLE 2 Nonspecific binding of cationic diamidines in mouse plasma and brain

Compound	Concn (μM)	% f_u (mean ± SD)[a] in: Plasma	Brain
Pentamidine	1	8.4 ± 1.2[b]	0.3 ± 0.1
	5	10 ± 1.2	0.5 ± 0.1
DB75	1	6.8 ± 0.7	0.1 ± 0.05
	5	8.0 ± 0.4	0.09 ± 0.01
DB820	1	21 ± 2.0	0.2 ± 0.05[c]
	5	19 ± 2.4	0.4 ± 0.06[c]
DB829	1	40 ± 8.2[b]	1.5 ± 0.3
	5	36 ± 3.3	1.4 ± 0.4

[a] f_u, drug unbound fraction. Results are from triplicate determinations.
[b] Previously published value (8).
[c] The difference between the results at 1 and 5 μM was statistically significant ($P < 0.05$).
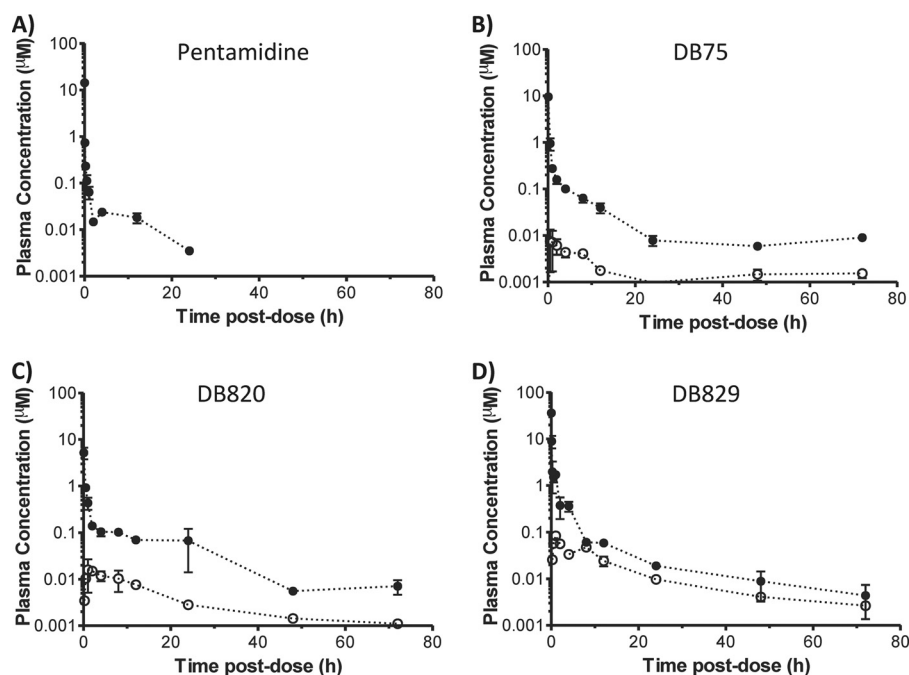
FIG 2 Plasma concentration-time profiles of cationic diamidines following intravenous (filled circles) or oral (open circles) administration to healthy mice. A single dose of pentamidine, DB75, DB820, or DB829 was administered i.v. (7.5 µmol/kg, or approximately 2.3 to 2.6 mg/kg) or p.o. (100 µmol/kg, or approximately 30 mg/kg) to male Swiss Webster mice. Symbols and error bars represent means and standard errors of triplicate determinations.

est systemic exposure ($AUC_{0-\infty} = 73.9$ µM · h and $C_{max} = 31.6$ µM) among the diamidines, whereas pentamidine and DB75 were the lowest. The terminal elimination half-life ($t_{1/2}$) also exhibited variability, ranging from approximately 21 h for DB829 to 42 h for DB820.

The total brain concentration of each diamidine was measured at 4, 12, and 72 h postdose. Similar to plasma, DB829 showed the highest total brain concentrations, ranging from 5.7 to 8.7 µM, whereas pentamidine had the lowest, ranging from 0.51 to 0.7 µM (Fig. 3A and D). DB75 and DB820 had intermediate total brain

concentrations of 1.2 to 2.8 µM and 2.1 to 4.6 µM, respectively (Fig. 3B and C). Compared to the corresponding plasma concentrations, all diamidines showed high brain-to-plasma (B/P) ratios. At 72 h postdose, DB829 had the highest B/P ratio, 114, followed by DB75, DB820, and pentamidine (Table 4). The B/P ratios increased as the time postdose increased from 4 h to 72 h, suggesting that it took longer than 12 h to reach equilibrium between brain and plasma, and hence, the B/P ratios at 72 h may be more representative of steady-state B/P ratios. Furthermore, DB829 had the greatest AUC in the brain, followed by DB820, DB75, and pent-

TABLE 3 Pharmacokinetic parameters of cationic diamidines after i.v. and p.o. administration to mice

Route	Parameter[a] (unit of measure)	Pentamidine[b]	DB75	DB820	DB829[b]
i.v.	Dose, [µmol/kg (mg/kg)]	7.5 (2.6)	7.5 (2.3)	7.5 (2.3)	7.5 (2.3)
	$C_{5\,min}$ (µmol/liter)	0.74 ± 0.21	9.6 ± 0.25	5.2 ± 2.5	9.0 ± 4.6
	$AUC_{0-\infty}$ (µmol/liter · h)	1.2	5.2	4.9	7.6
	$t_{1/2}$ (h)	7.2	58	24	18
	CL (liters/h/kg)	6.3	1.5	1.5	0.98
	V_{ss} (liters/kg)	23	41	23	7.1
	MRT (h)	3.6	28	15	7.2
p.o.	Dose [µmol/kg (mg/kg)]	ND	100 (30)	100 (30)	100 (30)
	C_{max} (µmol/liter)	ND	0.008	0.016	0.083
	T_{max} (h)	ND	0.5	1	1
	$AUC_{0-\infty}$ (µmol/liter · h)	ND	0.13[c]	0.31	1.01
	$t_{1/2}$ (h)	ND	107	26	21
	F (%)	ND	0.2	0.5	1.0

[a] Abbreviations: $C_{5\,min}$, plasma concentration at 5 min postdose; C_{max}, maximum plasma concentration; $t_{1/2}$, terminal elimination half-life; T_{max}, time to reach C_{max}; $AUC_{0-\infty}$, area under the plasma concentration-time curve from time zero to infinite time; CL, clearance; V_{ss}, steady-state volume of distribution; F, oral bioavailability; MRT, mean residence time; ND, not determined.

[b] The i.v. PK measurements for plasma were previously published (8).

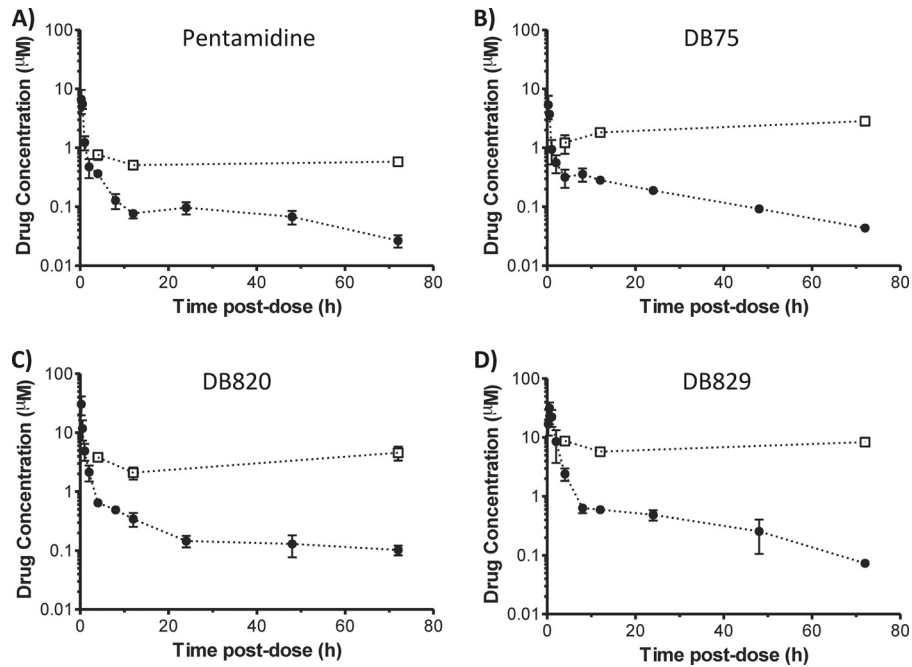[c] AUC was calculated for 0 to 72 h, as extrapolation beyond 72 h would account for >30% of total AUC.

FIG 3 Plasma (filled circles) and brain (open squares) concentration-time profiles of cationic diamidines following intraperitoneal administration to healthy mice. A single dose of pentamidine, DB75, DB820, or DB829 was administered i.p. (65 μmol/kg, or approximately 20 to 22 mg/kg) to male Swiss Webster mice. Symbols and error bars represent means and standard errors of triplicate determinations.

amidine (Table 4). In contrast, when plasma-to-brain unbound fraction ratios ($f_{u,plasma}/f_{u,brain}$) were compared, DB829 and pentamidine had the lowest ratios, whereas DB75 had the highest (Table 4).

Drug exposure-effect relationships. To explore the relationships between pharmacodynamics and different pharmacokinetic outcomes of cationic diamidines, drug effect (i.e., in vivo efficacy) was plotted against various definitions of drug exposure (Fig. 4 and 5). Relevant in vitro antitrypanosomal activities and in vivo efficacies of cationic diamidines (see Table S1 in the supplemental material) were previously published by Wenzler et al. (6). For first-stage HAT using the *T. b. rhodesiense* STIB900 acute mouse

model, drug efficacy was compared to plasma C_{max} and AUC, unbound plasma C_{max} and AUC, and IC_{50}-normalized unbound plasma C_{max} and AUC (Fig. 4). AUC-based measurements exhibited a straightforward relationship with drug effect (Fig. 4B, D, and F), which resembled the upper portion of a dose-response curve defined by the E_{max} model (22).

For second-stage HAT using the *T. b. brucei* GVR35 CNS mouse model, drug efficacy was compared to drug brain concentration and AUC, unbound brain concentration and AUC, and IC_{50}-normalized unbound brain concentration and AUC, as well as B/P ratio and unbound plasma-to-brain fraction ratio (Fig. 5). Because different dose regimens were used in the previous efficacy testing (see Table S1 in the supplemental material), DB75 drug exposures were dose corrected, assuming a linear dose-exposure relationship in the small dose range of 12.5 to 20 mg/kg. Although pentamidine was not directly tested at 10 doses of 20 mg/kg/day i.p. in the GVR35 CNS mouse model, it is reasonable to expect that it would not be curative at this dose, since 10 doses of 12.5 mg/kg/day was not curative (see Table S1). The results showed that there was, in general, a linear relationship between CNS efficacy and drug exposure. The B/P ratio showed the best correlation ($R^2 = 0.94$) with the CNS efficacy of all four cationic diamidines (Fig. 5G). The unbound brain concentration (Fig. 5C) and AUC (Fig. 5D) also gave good correlations ($R^2 = 0.94$); however, no definitive conclusion could be drawn due to the lack of data points for intermediate efficacy.

DISCUSSION

It is extraordinary that the cationic azadiamidine DB829 was able to completely cure mice and monkeys with second-stage HAT infections in spite of the long-held notion that cationic diamidines (positively charged at physiologic pH) lack the necessary passive

TABLE 4 Pharmacokinetic parameters of cationic diamidines after i.p. administration to mice

Parameter[a] (unit of measure)	Pentamidine[b]	DB75	DB820	DB829[b]
Dose [μmol/kg (mg/kg)]	65 (22)	65 (20)	65 (20)	65 (20)
C_{max} (μmol/liter)	6.66	5.33	30.5	31.6
$t_{1/2}$ (h)	34.4	21.9	41.7	21.2
T_{max} (h)	0.25	0.25	0.25	0.50
$AUC_{0-\infty}$ (μmol/liter · h)	10.7	15.9	37.2	73.9
C_{brain_72h} (μmol/liter)	0.579	2.84	4.55	8.35
AUC_{brain_0-72h} (μmol/liter · h)	39	169	275	508
B/P ratio at 72 h	22.8	65.5	44.5	114
$f_{u,plasma}/f_{u,brain}$[c]	23	74	67	25

[a] Abbreviations: C_{max}, maximum plasma concentration; $t_{1/2}$, terminal elimination half-life; T_{max}, time to reach C_{max}; $AUC_{0-\infty}$, area under the plasma concentration-time curve from time zero to infinite time; C_{brain_72h}, brain concentration at 72 h postdose; AUC_{brain_0-72h}, area under the brain concentration curve from time zero to 72 h postdose; B/P, brain-to-plasma concentration ratio; f_u, drug unbound fraction.
[b] The plasma PK measurements were previously published (8).
[c] The unbound fractions were averaged using values determined with final drug concentrations of 1 and 5 μM (Table 2).
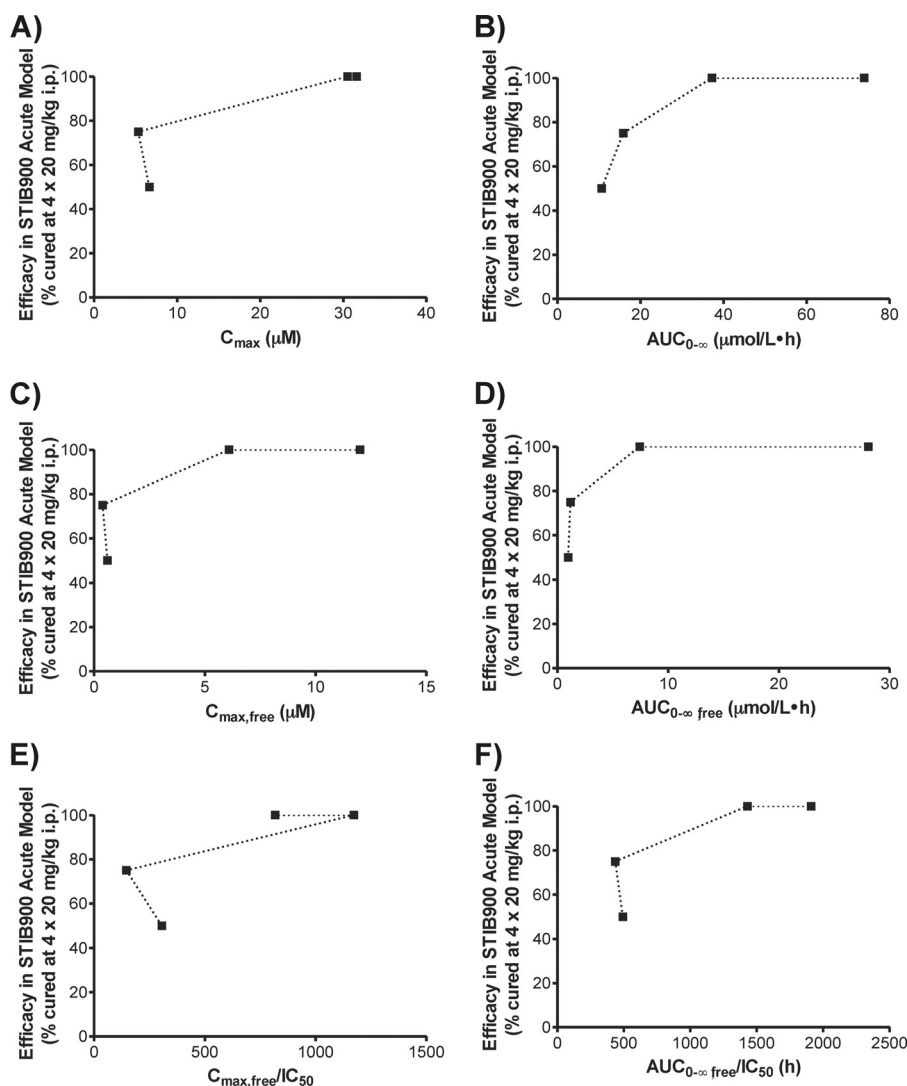
FIG 4 Drug exposure-effect relationships of cationic diamidines in the *T. b. rhodesiense* STIB900 acute mouse model. Dotted lines connect data points from pentamidine, DB75, DB820, and DB829, respectively. Relevant *in vitro* antitrypanosomal activities and *in vivo* efficacies of cationic diamidines were previously published by Wenzler et al. (6) and are summarized in Table S1 in the supplemental material.

permeability to traverse the BBB to kill trypanosomes residing in the CNS. Hence, a better understanding of the biochemical mechanisms underlying the differential efficacies of cationic diamidines is warranted to further assist in the development of diamidine-based chemotherapies against second-stage HAT. In this study, a pharmacokinetic characterization was conducted to compare the plasma and brain exposures of four representative cationic diamidines, pentamidine, DB75, DB820, and DB829, and to explore the relationship between drug exposure and effect.

All four diamidines showed a long microsomal half-life (Table 1), indicating that little metabolism occurred during incubation with mouse liver microsomes. Pentamidine was the least stable when the percentage of substrate remaining at the end of incubation ($t = 60$ min) was compared. Pentamidine was shown previously to be metabolized by rat liver microsomes and isolated perfused rat livers via hydrocarbon chain hydroxylation (major pathway) and amidine N-hydroxylation (minor pathway) (23). Hence, the replacement of the pentyl linker between two aromatic

amidine groups with a furan linker (Fig. 1) appears to have reduced the susceptibility to metabolism in mice, which could have contributed to the greater plasma AUC values observed for diamidines with a furan linker (Tables 3 and 4). In addition, these metabolically stable furan linkers are not expected to be mutagenic, as they did not pose this problem for pafuramidine (24) or antileishmanial arylimidamides (12).

In general, cationic diamidines had low levels of permeability (0.54×10^{-6} to 5.4×10^{-6} cm/s) across MDCK cell monolayers (Table 1), consistent with the notion that they lack the necessary passive permeability to efficiently cross either the enteric barrier or the BBB (25, 26). This was further supported by the extremely low oral bioavailability of cationic diamidines (F ≤ 1%) (Table 3). Nonetheless, there appeared to be an upward trend in oral absorption for the azadiamidines DB820 and DB829. For example, DB829 had 5-fold higher oral bioavailability than DB75 (1% versus 0.2%) and reached a maximal plasma concentration of 0.083 µM after a single oral dose of 100 µmol/kg (30 mg/kg) (Table 3).
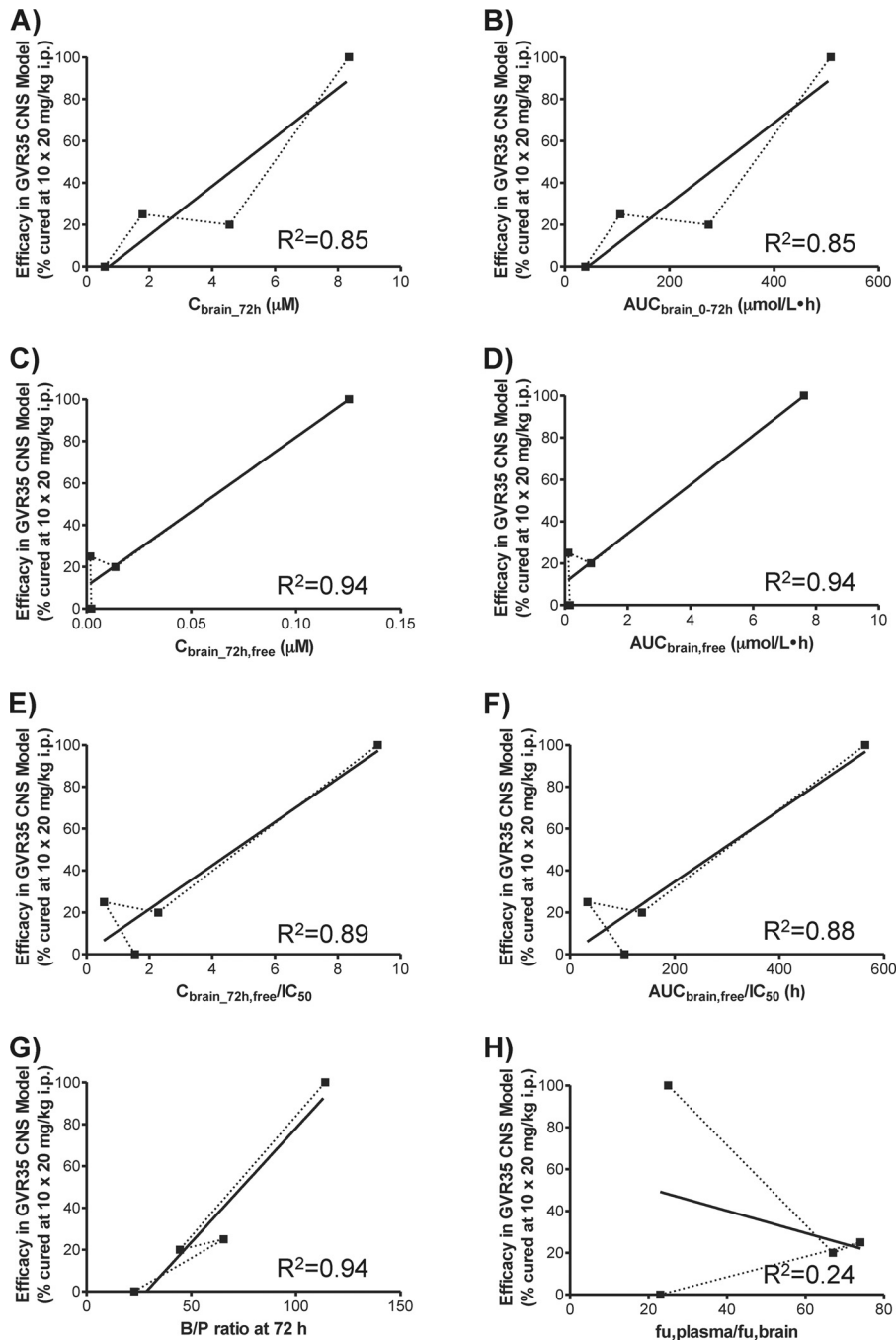
FIG 5 Drug exposure-effect relationships of cationic diamidines in the *T. b. brucei* GVR35 CNS mouse model. Dotted lines connect data points from pentamidine, DB75, DB820, and DB829, respectively. Solid lines represent least-square linear regressions. Relevant *in vitro* antitrypanosomal activities and *in vivo* efficacies of cationic diamidines were previously published by Wenzler et al. (6) and are summarized in Table S1 in the supplemental material.

This explains our previous observation that DB829, administered orally at 4 doses of 50 mg/kg/day, cured 3/4 mice with acute *T. b. rhodesiense* STIB900 infections (antitrypanosomal IC_{50} of 0.0147 μM for DB829) (8).

None of the diamidines examined appeared to be a substrate of the human MDR1 efflux transporter (Table 1), indicating that P-gp-mediated efflux was unlikely to be the cause of the differential CNS activity observed with the cationic diamidines. It is unknown whether these diamidines are substrates of the other hu-

man P-glycoprotein, MDR3, although there is little evidence that MDR3 plays a major role in the transport of drugs (27). However, pentamidine was shown previously to be a substrate of mouse P-gp (Mdr1a/b) via *in situ* brain perfusion of FVB Mdr1a/Mdr1b$^{-/-}$ knockout mice (5). These results suggest that the interaction of cationic diamidines with the P-gp efflux transporter is species dependent.

Each cationic diamidine differed markedly in its nonspecific binding to plasma proteins and brain tissues. Among the four

diamidines, DB75 bound most avidly to both plasma proteins and brain, whereas the azadiamidine DB829 showed the least binding (Table 2). The binding to brain greatly exceeded that to plasma proteins, by 23- to 74-fold (Fig. 5H), resulting in the apparent volumes of distribution being greater than the physiologic fluid volumes for the cationic diamidines (Table 3). Yan et al. (19) previously demonstrated that hepatic binding underlay the differences in systemic exposure of DB75 and DB829, which are both formed from their methamidoxime prodrugs (pafuramidine and DB868, respectively) in the rat liver. Hence, it can be postulated that binding to brain, as well as other tissues where diamidines distribute, could also underlie the differences in systemic exposure of the cationic diamidines when administered parenterally. This warrants further compartmental pharmacokinetic investigation once the binding of diamidines in other tissues is determined.

The activity of the cationic diamidines against acute *T. b. rhodesiense* STIB900 infections appeared to be more AUC dependent than C_{max} driven (Fig. 4). This is consistent with our previous observation (8) that the *in vitro* antitrypanosomal activity of DB829 did not increase with drug concentrations greater than 2 μM, likely due to the saturation of the P2 transporter-mediated uptake into trypanosomes. This property may prove to be desirable, because dosing regimens can be adjusted (e.g., longer or more frequent) to use lower doses for better safety, assuming toxicity is C_{max} driven. Although it appeared to have followed the dose-response curve defined by the E_{max} model (Fig. 4B, D, and F) (22), the drug exposure-effect relationship needs to be further defined using a pharmacokinetic-pharmacodynamic modeling approach with drug exposure and efficacy determined at multiple dose levels.

The activity of the cationic diamidines against CNS *T. b. brucei* GVR35 infections showed a good linear correlation with the B/P ratio at 72 h postdose (Fig. 5G). The B/P ratio, also known as the brain/plasma partition coefficient ($K_{p,brain}$), is the most widely used *in vivo* parameter to evaluate the extent of CNS penetration. A $K_{p,brain}$ of ≥1 often indicates "good" CNS penetration, while a $K_{p,brain}$ of ≪1 suggests "poor" CNS penetration (28); however, exceptions to this arbitrary $K_{p,brain}$ cutoff exist, such as the antipsychotic drug sulpiride (0.078) and the sedative midazolam (0.23) (29). Surprisingly, all cationic diamidines examined in this study showed high B/P ratios, ranging from 23 for pentamidine up to 114 for DB829 (Table 4), suggesting good CNS penetration. However, only DB829 cured mice with CNS *T. b. brucei* GVR35 infections (6). Using fluorescence microscopy, Sturk et al. (30) previously demonstrated that DB75 did not distribute into brain parenchyma. Instead, it was sequestered within endothelial cells lining the BBB and blood-cerebrospinal fluid (CSF) barrier. Hence, the B/P ratio alone is not a good predictor for CNS activity of cationic diamidines against second-stage HAT. Our results, however, showed that the B/P ratio could be used to rank cationic diamidines in terms of CNS activity within the same compound class.

The *in vitro* plasma-to-brain unbound fraction ratios ($f_{u,plasma}/f_{u,brain}$) did not correlate with the CNS activities of the cationic diamidines (Fig. 5H). Several papers have reported the use of the $f_{u,plasma}/f_{u,brain}$ ratio to predict the B/P ratio of CNS and non-CNS compounds (20, 29, 31, 32). Good agreement has been observed for compounds that do not exhibit active efflux at the BBB, whereas the $f_{u,plasma}/f_{u,brain}$ ratio overpredicted the B/P ratio for compounds that are actively effluxed (e.g., P-gp substrates). To account for P-gp-mediated efflux at the BBB, the $f_{u,plasma}/f_{u,brain}$ ratio was corrected using the efflux ratio and subsequently showed an improved correlation with the *in vivo* B/P ratio (32). However, since cationic diamidines are not subjected to P-gp-mediated efflux (Table 1), it is not expected that the efflux ratio correction would improve prediction of the *in vivo* B/P ratio by the *in vitro* $f_{u,plasma}/f_{u,brain}$ ratio.

The $f_{u,plasma}/f_{u,brain}$ ratio appears to have underpredicted the B/P ratio of the CNS-active DB829 (Table 4). This may be explained by preferential uptake of the azadiamidine DB829 via an uptake transporter(s) expressed at the apical (blood luminal) side of the BBB. Pentamidine and DB75 are good substrates for human organic cation transporter 1 (hOCT1) and weak substrates for hOCT2 but not for hOCT3 (33). hOCT1 is highly expressed in hepatocytes but not in the brain, whereas hOCT2 can be found in renal proximal tubules and neurons (34). The hOCT1-mediated hepatic sequestration of DB75 after intestinal absorption may contribute to its lower oral bioavailability compared to those of DB820 and DB829 (Table 3). However, it is unknown whether DB820 and DB829 also are substrates for these transporters, and the roles these transporters may have in mediating the uptake of diamidines into the CNS are largely unexplored. In addition, several trypanosomal transporters have been implicated in the uptake of cationic diamidines into trypanosomes. These include the P2 aminopurine transporter (TbAT1) (35–37) and aquaglyceroporin 2 (38). The P2 aminopurine transporter belongs to the nucleoside transporter family. In mammals, the nucleoside transporter family consists of three concentrative nucleoside transporters (CNTs) and four equilibrative nucleoside transporters (ENTs), which are expressed in the brain and various other tissues (39). It can be postulated that azadiamidines are substrates of mammalian nucleoside transporters and preferentially transported into the brain, which warrants future investigation.

In conclusion, pharmacokinetics (i.e., AUC, tissue binding, and CNS penetration) play an important role in determining the *in vivo* efficacies of cationic diamidines against first- and second-stage HAT. The azadiamidine DB829 showed higher systemic exposure, less tissue binding, and greater CNS penetration, which contributed to its excellent *in vivo* efficacy in animal models of both first- and second-stage HAT. Our results further support DB829 as a preclinical candidate for the treatment of second-stage HAT. In addition, better understanding of the uptake transport mechanisms of azadiamidines at the BBB will be important for defining the pharmacokinetic-pharmacodynamic relationship for antitrypanosomal diamidines, as well as for the brain uptake of CNS drugs in general.

ACKNOWLEDGMENT

REFERENCES

1. **Brun R, Don R, Jacobs RT, Wang MZ, Barrett MP.** 2011. Development of novel drugs for human African trypanosomiasis. Future Microbiol. **6:**677–691. http://dx.doi.org/10.2217/fmb.11.44.
2. **Brun R, Blum J, Chappuis F, Burri C.** 2010. Human African trypanosomiasis. Lancet **375:**148–159. http://dx.doi.org/10.1016/S0140-6736(09)60829-1.
3. **Simarro PP, Diarra A, Ruiz Postigo JA, Franco JR, Jannin JG.** 2011. The human African trypanosomiasis control and surveillance programme of the World Health Organization 2000-2009: the way forward. PLoS Negl. Trop. Dis. **5:**e1007. http://dx.doi.org/10.1371/journal.pntd.0001007.

4. **Dorlo TP, Kager PA.** 2008. Pentamidine dosage: a base/salt confusion. PLoS Negl. Trop. Dis. **2:**e225. http://dx.doi.org/10.1371/journal.pntd .0000225.

5. **Sanderson L, Dogruel M, Rodgers J, De Koning HP, Thomas SA.** 2009. Pentamidine movement across the murine blood-brain and blood-cerebrospinal fluid barriers: effect of trypanosome infection, combination therapy, P-glycoprotein, and multidrug resistance-associated protein. J. Pharmacol. Exp. Ther. **329:**967–977. http://dx.doi.org/10.1124/jpet.108 .149872.

6. **Wenzler T, Boykin DW, Ismail MA, Hall JE, Tidwell RR, Brun R.** 2009. New treatment option for second-stage African sleeping sickness: in vitro and in vivo efficacy of aza analogs of DB289. Antimicrob. Agents Chemother. **53:**4185–4192. http://dx.doi.org/10.1128/AAC.00225-09.

7. **Thuita JK.** 2013. Biological and pharmacological investigations of novel diamidines in animal models of human African trypanosomiasis. Ph.D. thesis. University of Basel, Basel, Switzerland.

8. **Wenzler T, Yang S, Braissant O, Boykin DW, Brun R, Wang MZ.** 2013. Pharmacokinetics, Trypanosoma brucei gambiense efficacy, and time of drug action of DB829, a preclinical candidate for treatment of second-stage human African trypanosomiasis. Antimicrob. Agents Chemother. **57:**5330–5343. http://dx.doi.org/10.1128/AAC.00398-13.

9. **Ismail MA, Brun R, Easterbrook JD, Tanious FA, Wilson WD, Boykin DW.** 2003. Synthesis and antiprotozoal activity of aza-analogues of furamidine. J. Med. Chem. **46:**4761–4769. http://dx.doi.org/10.1021 /jm0302602.

10. **Stephens C, Patrick DA, Chen H, Tidwell RR, Boykin DW.** 2001. Synthesis of deuterium-labelled 2,5-Bis(4-amidinophenyl)furan, 2,5-Bis[4-(methoxyamidino)phenyl]furan, and 2,7-diamidinocarbazole. J. Labelled Comp. Radiopharm. **44:**197–208. http://dx.doi.org/10.1002/jlcr .444.

11. **Avdeef A.** 2001. Physicochemical profiling (solubility, permeability and charge state). Curr. Top. Med. Chem. **1:**277–351. http://dx.doi.org/10 .2174/1568026013395100.

12. **Wang MZ, Zhu X, Srivastava A, Liu Q, Sweat JM, Pandharkar T, Stephens CE, Riccio E, Parman T, Munde M, Mandal S, Madhubala R, Tidwell RR, Wilson WD, Boykin DW, Hall JE, Kyle DE, Werbovetz KA.** 2010. Novel arylimidamides for treatment of visceral leishmaniasis. Antimicrob. Agents Chemother. **54:**2507–2516. http://dx.doi.org/10.1128 /AAC.00250-10.

13. **Wang MZ, Saulter JY, Usuki E, Cheung YL, Hall M, Bridges AS, Loewen G, Parkinson OT, Stephens CE, Allen JL, Zeldin DC, Boykin DW, Tidwell RR, Parkinson A, Paine MF, Hall JE.** 2006. CYP4F enzymes are the major enzymes in human liver microsomes that catalyze the O-demethylation of the antiparasitic prodrug DB289 [2,5-bis(4-amidinophenyl)furan-bis-O-methylamidoxime]. Drug Metab. Dispos. **34:**1985–1994. http://dx.doi.org/10.1124/dmd.106.010587.

14. **Garberg P, Ball M, Borg N, Cecchelli R, Fenart L, Hurst RD, Lindmark T, Mabondzo A, Nilsson JE, Raub TJ, Stanimirovic D, Terasaki T, Oberg JO, Osterberg T.** 2005. In vitro models for the blood-brain barrier. Toxicol. In Vitro **19:**299–334. http://dx.doi.org/10.1016/j.tiv.2004.06.011.

15. **Hakkarainen JJ, Jalkanen AJ, Kaariainen TM, Keski-Rahkonen P, Venalainen T, Hokkanen J, Monkkonen J, Suhonen M, Forsberg MM.** 2010. Comparison of in vitro cell models in predicting in vivo brain entry of drugs. Int. J. Pharm. **402:**27–36. http://dx.doi.org/10.1016/j.ijpharm .2010.09.016.

16. **Passeleu-Le Bourdonnec C, Carrupt PA, Scherrmann JM, Martel S.** 2013. Methodologies to assess drug permeation through the blood-brain barrier for pharmaceutical research. Pharm. Res. **30:**2729–2756. http://dx .doi.org/10.1007/s11095-013-1119-z.

17. **Troutman MD, Thakker DR.** 2003. Novel experimental parameters to quantify the modulation of absorptive and secretory transport of compounds by P-glycoprotein in cell culture models of intestinal epithelium. Pharm. Res. **20:**1210–1224. http://dx.doi.org/10.1023/A:1025001131513.

18. **US Food and Drug Administration.** 2006. Guidance for industry: drug interaction studies—study design, data analysis, and implications for dosing and labeling. Center for Drug Evaluation and Research, US FDA, Silver Spring, MD. http://www.fda.gov/Drugs/DevelopmentApprovalProcess /DevelopmentResources/DrugInteractionsLabeling/ucm093606.htm.

19. **Yan GZ, Brouwer KL, Pollack GM, Wang MZ, Tidwell RR, Hall JE, Paine MF.** 2011. Mechanisms underlying differences in systemic exposure of structurally similar active metabolites: comparison of two preclinical hepatic models. J. Pharmacol. Exp. Ther. **337:**503–512. http://dx.doi.org /10.1124/jpet.110.177220.

20. **Kalvass JC, Maurer TS.** 2002. Influence of nonspecific brain and plasma binding on CNS exposure: implications for rational drug discovery. Biopharm. Drug Dispos. **23:**327–338. http://dx.doi.org/10.1002/bdd.325.

21. **Chiou WL.** 1978. Critical evaluation of the potential error in pharmacokinetic studies of using the linear trapezoidal rule method for the calculation of the area under the plasma level-time curve. J. Pharmacokinet. Biopharm. **6:**539–546. http://dx.doi.org/10.1007/BF01062108.

22. **Macdougall J.** 2006. Analysis of dose-response studies—E_{max} model, p 127–145. In Ting N (ed), Dose finding in drug development. Statistics for Biology and Health. Springer, New York, NY.

23. **Berger BJ, Naiman NA, Hall JE, Peggins J, Brewer TG, Tidwell RR.** 1992. Primary and secondary metabolism of pentamidine by rats. Antimicrob. Agents Chemother. **36:**1825–1831. http://dx.doi.org/10.1128/AAC .36.9.1825.

24. **Paine MF, Wang MZ, Generaux CN, Boykin DW, Wilson WD, De Koning HP, Olson CA, Pohlig G, Burri C, Brun R, Murilla GA, Thuita JK, Barrett MP, Tidwell RR.** 2010. Diamidines for human African trypanosomiasis. Curr. Opin. Investig. Drugs **11:**876–883.

25. **Irvine JD, Takahashi L, Lockhart K, Cheong J, Tolan JW, Selick HE, Grove JR.** 1999. MDCK (Madin-Darby canine kidney) cells: a tool for membrane permeability screening. J. Pharm. Sci. **88:**28–33. http://dx.doi .org/10.1021/js9803205.

26. **Wager TT, Chandrasekaran RY, Hou X, Troutman MD, Verhoest PR, Villalobos A, Will Y.** 2010. Defining desirable central nervous system drug space through the alignment of molecular properties, in vitro ADME, and safety attributes. ACS Chem. Neurosci. **1:**420–434. http://dx .doi.org/10.1021/cn100007x.

27. **Klaassen CD, Aleksunes LM.** 2010. Xenobiotic, bile acid, and cholesterol transporters: function and regulation. Pharmacol. Rev. **62:**1–96. http://dx .doi.org/10.1124/pr.109.002014.

28. **Kalvass JC, Maurer TS, Pollack GM.** 2007. Use of plasma and brain unbound fractions to assess the extent of brain distribution of 34 drugs: comparison of unbound concentration ratios to in vivo p-glycoprotein efflux ratios. Drug Metab. Dispos. **35:**660–666. http://dx.doi.org/10.1124 /dmd.106.012294.

29. **Doran A, Obach RS, Smith BJ, Hosea NA, Becker S, Callegari E, Chen C, Chen X, Choo E, Cianfrogna J, Cox LM, Gibbs JP, Gibbs MA, Hatch H, Hop CE, Kasman IN, Laperle J, Liu J, Liu X, Logman M, Maclin D, Nedza FM, Nelson F, Olson E, Rahematpura S, Raunig D, Rogers S, Schmidt K, Spracklin DK, Szewc M, Troutman M, Tseng E, Tu M, Van Deusen JW, Venkatakrishnan K, Walens G, Wang EQ, Wong D, Yasgar AS, Zhang C.** 2005. The impact of P-glycoprotein on the disposition of drugs targeted for indications of the central nervous system: evaluation using the MDR1A/1B knockout mouse model. Drug Metab. Dispos. **33:**165–174. http://dx.doi.org/10.1124/dmd.104.001230.

30. **Sturk LM, Brock JL, Bagnell CR, Hall JE, Tidwell RR.** 2004. Distribution and quantitation of the anti-trypanosomal diamidine 2,5-bis(4-amidinophenyl)furan (DB75) and its N-methoxy prodrug DB289 in murine brain tissue. Acta Trop. **91:**131–143. http://dx.doi.org/10.1016/j .actatropica.2004.03.010.

31. **Maurer TS, Debartolo DB, Tess DA, Scott DO.** 2005. Relationship between exposure and nonspecific binding of thirty-three central nervous system drugs in mice. Drug Metab. Dispos. **33:**175–181. http://dx.doi.org /10.1124/dmd.104.001222.

32. **Summerfield SG, Stevens AJ, Cutler L, del Carmen Osuna M, Hammond B, Tang SP, Hersey A, Spalding DJ, Jeffrey P.** 2006. Improving the in vitro prediction of in vivo central nervous system penetration: integrating permeability, P-glycoprotein efflux, and free fractions in blood and brain. J. Pharmacol. Exp. Ther. **316:**1282–1290. http://dx.doi.org/10.1124 /jpet.105.092916.

33. **Ming X, Ju W, Wu H, Tidwell RR, Hall JE, Thakker DR.** 2009. Transport of dicationic drugs pentamidine and furamidine by human organic cation transporters. Drug Metab. Dispos. **37:**424–430. http://dx .doi.org/10.1124/dmd.108.024083.

34. **Giacomini KM, Huang SM, Tweedie DJ, Benet LZ, Brouwer KL, Chu X, Dahlin A, Evers R, Fischer V, Hillgren KM, Hoffmaster KA, Ishikawa T, Keppler D, Kim RB, Lee CA, Niemi M, Polli JW, Sugiyama Y, Swaan PW, Ware JA, Wright SH, Yee SW, Zamek-Gliszczynski MJ, Zhang L, International Transporter Consortium.** 2010. Membrane transporters in drug development. Nat. Rev. Drug Discov. **9:**215–236. http://dx.doi.org /10.1038/nrd3028.

35. **Carter NS, Berger BJ, Fairlamb AH.** 1995. Uptake of diamidine drugs by the P2 nucleoside transporter in melarsen-sensitive and -resistant

Trypanosoma brucei brucei. J. Biol. Chem. **270:**28153–28157. http://dx .doi.org/10.1074/jbc.270.47.28153.

36. **Lanteri CA, Stewart ML, Brock JM, Alibu VP, Meshnick SR, Tidwell RR, Barrett MP.** 2006. Roles for the Trypanosoma brucei P2 transporter in DB75 uptake and resistance. Mol. Pharmacol. **70:**1585–1592. http://dx .doi.org/10.1124/mol.106.024653.

37. **Ward CP, Wong PE, Burchmore RJ, de Koning HP, Barrett MP.** 2011. Trypanocidal furamidine analogues: influence of pyridine nitrogens on trypanocidal activity, transport kinetics, and resistance patterns. Antimicrob. Agents Chemother. **55:**2352–2361. http://dx.doi.org/10.1128/AAC .01551-10.

38. **Munday JC, Eze AA, Baker N, Glover L, Clucas C, Aguinaga Andres D, Natto MJ, Teka IA, McDonald J, Lee RS, Graf FE, Ludin P, Burchmore RJ, Turner CM, Tait A, Macleod A, Maser P, Barrett MP, Horn D, De Koning HP.** 2014. Trypanosoma brucei aquaglyceroporin 2 is a high-affinity transporter for pentamidine and melaminophenyl arsenic drugs and the main genetic determinant of resistance to these drugs. J. Antimicrob. Chemother. **69:**651–663. http://dx.doi.org/10 .1093/jac/dkt442.

39. **King AE, Ackley MA, Cass CE, Young JD, Baldwin SA.** 2006. Nucleoside transporters: from scavengers to novel therapeutic targets. Trends Pharmacol. Sci. **27:**416–425. http://dx.doi.org/10.1016/j.tips.2006.06.004.